Transport properties of monolayer and bilayer graphene p–n junctions with charge puddles in the quantum Hall regime

2010 J. Phys.: Condens. Matter 22 465301

(http://iopscience.iop.org/0953-8984/22/46/465301)

IOP Publishing Journal of Physics: Condensed Matter

J. Phys.: Condens. Matter **22** (2010) 465301 (8pp) doi:10.1088/0953-8984/22/46/465301

Transport properties of monolayer and bilayer graphene p–n junctions with charge puddles in the quantum Hall regime

Shu-guang Cheng

Department of Physics, Northwest University, Xi'an 710069, People's Republic of China

E-mail: sgcheng@nwu.edu.cn

Received 24 June 2010, in final form 28 September 2010
Published 29 October 2010
Online at stacks.iop.org/JPhysCM/22/465301

Abstract

Recent experiments have confirmed that the electron–hole inhomogeneity in graphene is a new type of charge disorder. Motivated by such confirmation, we theoretically study the transport properties of a monolayer graphene (MLG) based p–n junction and a bilayer graphene (BLG) p–n junction in the quantum Hall regime where electron–hole puddles are considered. By using the non-equilibrium Green function method, both the current and conductance are obtained. We find that, in the presence of the electron–hole inhomogeneity, the lowest quantized conductance plateau at e^2/h emerges in the MLG p–n junction under very small charge puddle disorder strength. For a BLG p–n junction, however, the conductance in the p–n region is enhanced with charge puddles, and the lowest quantized conductance plateau emerges at $2e^2/h$. Besides, when an ideal quantized conductance plateau is formed for a MLG p–n junction, the universal conductance fluctuation is found to be $2e^2/3h$. Furthermore, we also investigate the influence of Anderson disorder on such p–n junctions and the comparison and discussion are given accordingly. To compare the two models with different types of disorder, we investigate the conductance distribution specially. Finally the influence of disorder strength on the conductance of a MLG p–n junction is investigated.

(Some figures in this article are in colour only in the electronic version)

1. Introduction

Research on graphene is one of the most attractive topics in condensed matter physics nowadays. Graphene, which was first fabricated in 2004, is an ideal two-dimensional material with peculiar electronic properties [1]. In graphene, electrons behave like massless fermions [2] and are described by the massless Dirac relativistic equation with linear energy dispersion in the vicinity of Dirac points [3]. Many interesting phenomena are due to such a unique energy band structure, such as relativistic Klein tunneling [4] and Veselago lensing [5] in a monolayer graphene (MLG) p–n junction [6]. The MLG p–n junction can be realized in a graphene nanoribbon with two terminals electron- and hole-doped respectively by applying a gate voltage. The quantum Hall conductance in graphene is $G = (4n + 2)e^2/h$ with filling factor $\nu = (4n + 2)$ and $n = 0, \pm1, \pm2 \ldots$ [7]. The degeneracy 4 comes from the number of spins and valleys and 2 is contributed by the Landau level located at zero energy. These quantized Hall plateaus can be observed even at room temperature, and thus graphene is a good candidate for quantum computation and spintronics devices [8]. For the bilayer graphene (BLG), however, the band structure as well as electron transport properties are very different from those of MLG [9]. BLG is described by chiral quasiparticles with a parabolic dispersion at low energy [10, 11]. Besides, the Berry phase of BLG is 2π, in contrast to π in MLG, and has been confirmed by the quantum Hall effect [7, 11]. Moreover, the quantum Hall conductance of BLG is $4ne^2/h$ with $n = \pm1, \pm2, \pm3 \ldots$.

Recently, experiments have shown that new quantized conductance plateaus can be found in an MLG p–n junction

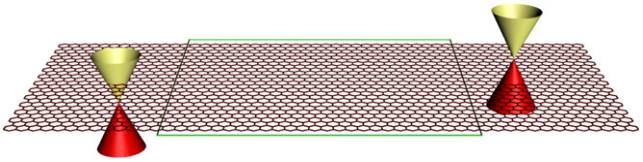

Figure 1. Schematic diagram for a zigzag edged MLG p–n junction. The left part is p-doped while the right part is n-doped, which can be controlled by a gate voltage. The middle rectangular area is the central region connecting the two parts. The potential in the central area is assumed to be the combination of a slope along the ribbon edge and electron–hole inhomogeneity depicted by figure 2.

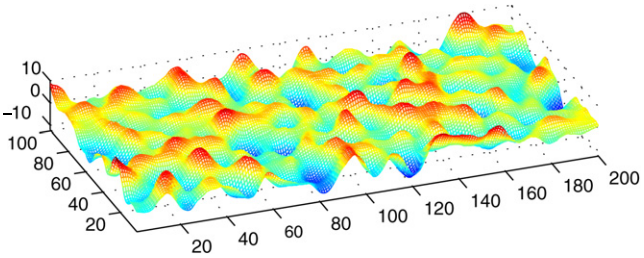

Figure 2. Electron–hole puddles in MLG generated by equation (3). The red parts (packets) and blue parts (dips) are electron puddles and hole puddles, respectively.

with $G = \frac{e^2}{h}\frac{|\nu_p||\nu_n|}{|\nu_p|+|\nu_n|}$, in which ν_p, ν_n are the filling factors in the p and n regions, respectively [12]. For instance, if $\nu_p = 2$ and $\nu_n = 2$, the corresponding G is e^2/h. Soon afterward, several theoretical works gave explanations of these results and showed that such anomalous quantized conductance plateaus should be attributed to charge disorder [13, 14]. Long and coworkers found that in the presence of Anderson disorder, conductance is strongly enhanced in an MLG p–n junction and this result agrees with the experiment well. Specifically, under Anderson disorder, the mixture of electron and hole Hall edge modes is largely strengthened at the p–n boundary. Consequently, the transport of carriers from electron (hole) doped terminals to hole (electron) doped terminals is facilitated by disorder as required by the band selective rule. Very recently, Liao *et al* have studied the quantized conductance plateau in inhomogeneous bilayer graphene in the quantum Hall regime and they found the anomalous quantized conductance plateau as a result of mixture quantum states from different Landau levels [15]. Klein tunneling, an effect first discovered in the field of high energy physics, is an important ingredient for electron transport in the graphene p–n junction. It distinguishes graphene from ordinary electronic materials. Under electron–hole inhomogeneity, however, Klein tunneling will be suppressed [16]. So the competition between Klein tunneling and the band selective rule dictates the transport properties of graphene.

Charge disorder is an important sort of disorder in graphene. Local changing of on-site energies of carbon atoms induces significant variation of the density of states and different characters of transport properties [17]. Very recently it was reported in experiment that electron–hole inhomogeneity, or charge puddles, exists in graphene [18]. With charge puddles, electrons or holes are aggregated in the short range and randomly distributed in the long range. The existence of charge inhomogeneity may be responsible for the minimum conductance in graphene [19]. In graphene, the heights of the electron–hole puddles are approximately 30 meV in energy space. Besides, it is also reported that charge puddles are found in bilayer graphene (BLG) [20]. Similar to the Anderson disorder, charge puddles can also mix the electron Hall edge states and hole Hall edge states. Consequently it occurs to us to ask whether charge puddles can induce quantized conductance plateaus in MLG p–n junctions. If so, then what is the differences between a charge puddle disorder and Anderson disorder? In addition, what is the influence of a charge puddle in a BLG p–n junction? A detailed theoretical investigation is needed.

In this paper, we theoretically study an MLG based p–n junction and a BLG p–n junction under a perpendicular magnetic field B where electron–hole puddles are considered to be in the central region (see figures 1 and 2). By using the non-equilibrium Green function method, the conductances are obtained. In the presence of an electron–hole inhomogeneity, we find that the conductance of an MLG p–n junction is strongly enhanced under very small charge puddle disorder strength (typically of the value 30 meV in experiment) [18]. A new quantized conductance emerges at e^2/h and the fluctuation of conductance is also found to form a plateau at $2e^2/3h$. For the BLG p–n junction, however, the conductance is enhanced under charge puddles, and the conductance plateau emerges at $2e^2/h$. The enhancement of conductance in the charge puddle model has several similarities with the Anderson disorder model as well as some differences. Thus we also investigate the conductance distribution in p–n junctions for both MLG and BLG cases where charge puddle disorder and Anderson disorder are considered. We find that when an ideal quantized conductance plateau is formed, the conductance is subject to a Gaussian distribution in both cases. On the other hand, when the conductance value is not an ideal one, the conductances distribution is of a particular symmetric distribution with the symmetric center at ne^2/h with n being integer. Finally we discuss the influence of puddle disorder on the conductance of an MLG p–n junction.

The rest of this paper is organized as follows. In section 2, we give the tight-binding Hamiltonian of the MLG and BLG p–n junctions with electron–hole inhomogeneity, the Keldysh non-equilibrium Green function method for deduction of the current and conductance expression, and also corresponding parameters. Numerical results and detailed discussions are given in section 3, including the conductance and conductance fluctuation of the MLG p–n junction and BLG p–n junction with electron–hole inhomogeneity. The distribution of conductances is discussed as well in two situations: with and without external magnetic field. Finally we investigate the conductance of an MLG p–n junction as a function of puddle disorder strength. We summarize our results in section 4.

2. The model and Hamiltonian

The model we considered is a p–n junction with zigzag edges for either the MLG (see figure 1) or the BLG case. The Hamiltonian of an MLG p–n junction in the tight-binding representation can be described by [14]

$$H_G = \sum_i \varepsilon_i a_i^\dagger a_i - \sum_{\langle ij\rangle} t a_i^\dagger a_{j\sigma} \mathrm{e}^{\mathrm{i}\varphi_{ij}} \tag{1}$$

where $a_i^\dagger$ (a_i) is the creation (annihilation) operator at the site i and $\varepsilon_i = \varepsilon_\mathrm{L}, \varepsilon_\mathrm{R}$ are the on-site energy at the left and right graphene terminal, respectively. The summation index $\langle ij\rangle$ counts the nearest hopping term. t is the nearest neighbor hopping energy and $\mathrm{e}^{\mathrm{i}\varphi_{ij}}$ represents the extra phase of hopping term induced by the perpendicular magnetic field. The relation between φ_{ij} and the vector potential $\vec{A}$ is $\varphi_{ij} = \frac{1}{\Phi_0}\int_i^j \vec{A}\cdot\mathrm{d}\vec{l}$ with $\Phi_0 = \hbar/e$ being the quantum magnetic flux. For a BLG p–n junction, the Hamiltonian in the tight-binding representation is

$$\begin{aligned} H_G = &\sum_k \varepsilon_i a_i^\dagger a_i + \sum_k \varepsilon_i b_i^\dagger b_i \\ &- \sum_{\langle ij\rangle} t a_i^\dagger a_j \mathrm{e}^{\mathrm{i}\varphi_{ij}} - \sum_{\langle ij\rangle} t b_i^\dagger b_j \mathrm{e}^{\mathrm{i}\varphi_{ij}} \\ &- \sum_{\langle ij\rangle} t_v (a_i^\dagger b_j + b_i^\dagger a_j) \end{aligned} \tag{2}$$

where a_i and b_i are annihilation operators of the two layers respectively and t_v is the interlayer coupling element. The electron–hole inhomogeneity is only considered in the central region (illustrated in the rectangular region in figure 1). The size of the central region is described by the width M and length N, which results in $2M(2N+1)$ carbon atoms in the central region for MLG and double that for BLG. For instance, the width of the nanoribbon $M = 30$ corresponds to $(3M-1)\times 0.142 \approx 12.64$ nm and the length of the central area is $\sqrt{3}M \approx 12.3$ nm for $N = 50$. The on-site energies in the central region ε_i are the combination of the charge puddles potential and a linear potential descending from one terminal to another, $\varepsilon_i = \varepsilon_\mathrm{L} + n(\varepsilon_\mathrm{R} - \varepsilon_\mathrm{L})/(2N+2) + \xi_i$ where $n = 1, 2, 3, \ldots, 2N+1$ is the length index along the edges in the central region and $2N+1$ is the total length of the central region. The electron–hole inhomogeneity is represented by ξ_i in the central region (see figure 2). Its value on site i is decided by [25]

$$\xi_i = \frac{\sum_j \xi_j \exp\left(-|\mathbf{r}_{ij}|^2/2\eta^2\right)}{\sqrt{\sum_j \exp\left(-|\mathbf{r}_{ij}|^2/\eta^2\right)}} \tag{3}$$

where η is the spatial correlation parameter, $|\mathbf{r}_{ij}|$ is the distance between sites i and j and the summation is over all carbon atoms in the central area. Here ξ_j is the uncorrelated on-site energy subject to a Gaussian distribution with zero mean and a variance W.[1] In the case of Anderson disorder, ξ_i in the center region is set as a uniform random distribution $[-W/2, W/2]$.

[1] The correlated on-site energy ε_i is generated in a square lattice, and we map it into a honeycomb lattice. Considering that the size of the puddles is much larger than the honeycomb lattice constant, the approximation is acceptable.

Using the Heisenberg equation of motion, the current flowing through the junction is [21]

$$I = \frac{2e}{\hbar}\int \frac{\mathrm{d}E}{2\pi}[f_\mathrm{L}(E) - f_\mathrm{R}(E)]T(E) \tag{4}$$

where $f_{\mathrm{L/R}}(E) = 1/\{\exp[(E - eV_{\mathrm{L/R}})/k_\mathrm{B}T]+1\}$ is the Fermi distribution in the left/right MLG terminal. In equation (4), $T(E) = \mathrm{Tr}\{\mathbf{\Gamma_L G^r \Gamma_R G}^a\}$ is the transmission coefficient from the left terminal to the right terminal. The retarded and advanced Green functions of the central region are defined by

$$\begin{aligned} \mathbf{G}^\mathrm{r}(E) &= \mathbf{G}^{a\dagger}(E) \\ &= (E\mathbf{I} - \mathbf{H}_\mathrm{c} - \mathbf{\Sigma}_\mathrm{L}^\mathrm{r} - \mathbf{\Sigma}_\mathrm{R}^\mathrm{r})^{-1}. \end{aligned} \tag{5}$$

Here $\mathbf{H}_\mathrm{c}$ is the Hamiltonian of the central region, as labeled by a rectangular area in figure 1 for the MLG case, and $\mathbf{I}$ is the identity matrix with the same dimension as $\mathbf{H}_\mathrm{c}$. The coupling of the central region to terminal α is accounted for by the retarded self-energy $\mathbf{\Sigma}_\alpha^\mathrm{r}(E) = t g_{\alpha,ij}^\mathrm{r}(E) t^*$, where $g_{\alpha,ij}^\mathrm{r}(E)$ is the surface Green function of terminal α. The linewidth function $\mathbf{\Gamma}_\alpha(E)$ can be defined with the aid of the self-energy $\mathbf{\Gamma}_\alpha(E) = \mathrm{i}[\mathbf{\Sigma}_\alpha^\mathrm{r} - (\mathbf{\Sigma}_\alpha^\mathrm{r})^\dagger]$. The surface Green functions of the infinite MLG and BLG terminals can be obtained by a standard numerical calculation procedure [22].

In the numerical calculation, we set the temperature at zero and thus the conductance can be obtained easily by $G(E) = \frac{\mathrm{d}I}{\mathrm{d}V}|_{V_\mathrm{L}=V_\mathrm{R}=0} = \frac{2e^2}{h}T(E)$. The conductance fluctuation is defined as $\delta G = \sqrt{\langle G^2\rangle - \langle G\rangle^2}$ where $\langle G\rangle$ is the average of G over the disorder configurations for a specific W. The perpendicular magnetic field is accounted for by adopting $\varphi = 0.007$ which is large enough for the formation of edge states[2]. The nearest neighbor hopping element $t \approx 2.75$ eV is adopted as the energy unit and the interlayer hopping element $t_v = 0.1t$ is chosen according to experiment [23].

In the following calculation, in the presence of electron–hole inhomogeneity or the Anderson disorder, both the conductance and conductance fluctuation are averaged over up to 1000 random configurations. While in the conductance distribution calculation, there are 5000 random configurations. Specially, in case of charge puddles inhomogeneity, we choose $W \approx 30$ meV, which is consistent with the typical experimental value of electron or hole puddle strength [18]. In equations (3) the spatial correlation parameter is set as 12.5 such that the size of puddle is approximately 3 nm [24].

3. Numerical results and discussion

3.1. MLG p–n junction with charge puddles

For a clean MLG p–n junction, the conductance G is a perfect quantized plateau in the p–p region or n–n region with $G = \frac{e^2}{h}\min\{|\nu_\mathrm{L}|, |\nu_\mathrm{R}|\}$ in which $\nu_{\mathrm{L/R}}$ is the filling factor of the left/right terminal [13, 14]. In the p–n or n–p region, G is quite small. Especially, if the length N is large, G is very small

[2] $\varphi = 0.007$ corresponds to $B \approx 170$ T, which is quite a large magnetic field. However, as we considered a small size sample, a strong magnetic field guarantees that the magnetic length is far smaller than the width of graphene ribbon. In the case of a large system, the magnetic field can be greatly decreased and the numerical results remain the same.

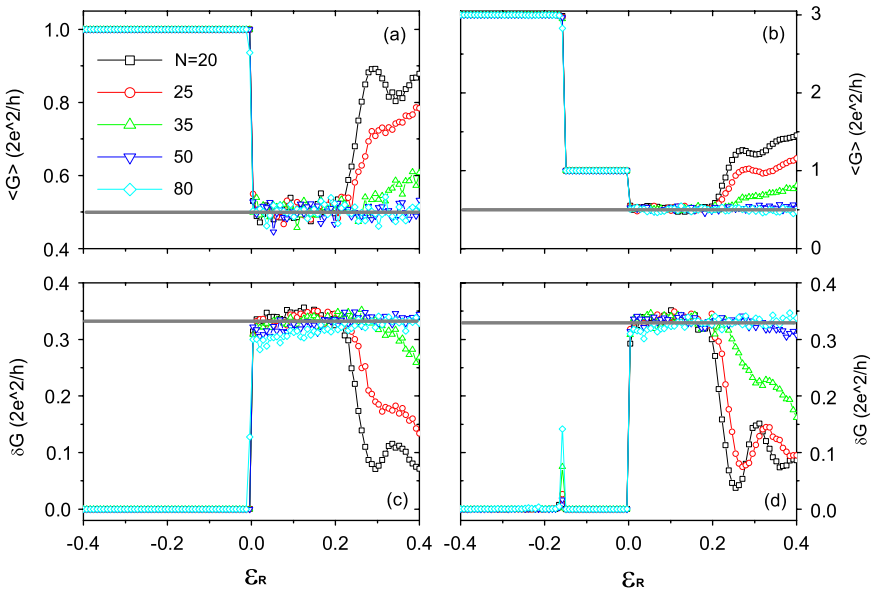

Figure 3. $\langle G\rangle$ ((a) and (b)) and δG ((c) and (d)) versus ε_R with electron–hole inhomogeneity $W = 30$ meV and $\varphi = 0.007$ in an MLG p–n junction for different lengths N ($M = 30$). Here two sets of ε_L parameters are adopted: $\varepsilon_L = -0.1$ ((a) and (c)) and $\varepsilon_L = -0.2$ ((b) and (d)). The gray lines indicate 0.5 in (a) and (b) and 1/3 for (c) and (d).

because of the weakened Klein tunneling. When considering the Anderson disorder at a proper strength, the conductance is strongly enhanced and a conductance plateau can be observed at $\langle G\rangle = \frac{e^2}{h}\frac{|\nu_L||\nu_R|}{|\nu_L|+|\nu_R|}$.

In the following we investigate the average conductance $\langle G\rangle$ and the fluctuation of conductance δG of an MLG p–n junction under electron–hole inhomogeneity in the central region. In figure 3 we show the results for $\varepsilon_L = 0.1$ ((a) and (c)) and $\varepsilon_L = 0.2$ ((b) and (d)). In the n–n region ($\varepsilon_L, \varepsilon_R < 0$), G is an integer times $2e^2/h$ given by $\langle G\rangle = \frac{e^2}{h}\min\{|\nu_L|, |\nu_R|\}$. Meanwhile in the p–n region ($\varepsilon_R > 0$) of a short p–n junction, the lowest quantized conductance plateau can be realized at e^2/h if one of the filling factors $|\nu_L|$ or $|\nu_R|$ is low (see figures 3(a) and (b) e.g. $N = 20, 30, 50$). If both filling factors $|\nu_L|, |\nu_R|$ are high (e.g. $|\nu_L| = |\nu_R| = 6$), $\langle G\rangle$ is larger than e^2/h and no conductance plateau can be realized. The longer the central area becomes, the smaller the conductance becomes as a result of the elimination of Klein tunneling. However, for a long p–n junction (e.g. $N = 80$), the conductance plateau at e^2/h can survive all the time. In figures 3(c) and (d), the fluctuation of conductance δG is almost zero in the n–n region except for the point at which the filling factor ν_R changes from -6 to -2. In a p–n junction, if a conductance plateau of $\langle G\rangle$ is formed, a universal conductance fluctuation is also observed and δG forms a plateau at $2e^2/3h$. However, for a short p–n junction and high filling factors $|\nu_L|$ and $|\nu_R|$, δG does not remain quantized and its value is less than $2e^2/3h$.

These results are partially different from that in an MLG p–n junction with Anderson disorder in three main aspects. (i) With electron–hole inhomogeneity, the lowest quantized conductance plateau can be realized with rather small disorder parameter, e.g. $W = 20$ meV $< 0.01t$ (see figure 9). However, the conductance plateau in an Anderson disorder model is realized with $W > 0.1$ [13, 14]. (ii) The lowest quantized conductance plateau emerges at high filling factors and small disorder strength. In an Anderson disorder model, the quantized conductance plateau is realized at high filling factors only for large disorder parameter (e.g. $W > 1$) [13]. (iii) In a long MLG p–n junction, the plateau of δG is formed in the charge puddle model at $2e^2/3h$, in contrast to the value of $e^2/\sqrt{3}h$ in the Anderson disorder model at the lowest filling factors.

The similarity and difference behaviors of the quantized conductance plateau in an Anderson disorder model and a charge puddle model can be explained as follows. In a tight-binding model, the hopping matrix element $t = \hbar^2/2m^*a^2$ is related to the lattice constant a. For a charge puddle model, however, the on-site energies of carbon atoms are subject to a Gaussian distribution. In real space, the on-site energies are correlated in short range and random in long range, while for an Anderson disorder model, the on-site energies are of uniform distribution and randomly distributed in real space both in short range and long range. Thus a small charge puddle disorder strength corresponds to an Anderson disorder model with relatively large W. Such results indicate that an electron–hole puddle can make the complete mixture of the electron and hole Hall states easier and hence transport through the junction can be easily realized. As a result, the lowest quantized conductance plateau in the p–n region can be realized with rather small charge puddle disorder strength.

3.2. BLG p–n junction with charge puddles

Next we investigate a BLG p–n junction. In figure 4, we show the G versus E in a clean BLG p–n junction for different lengths N and magnetic fields φ. When $\varphi = 0$, the quantized conductance is realized in the n–n region, while in the p–n regime, the conductance is large (generally larger than

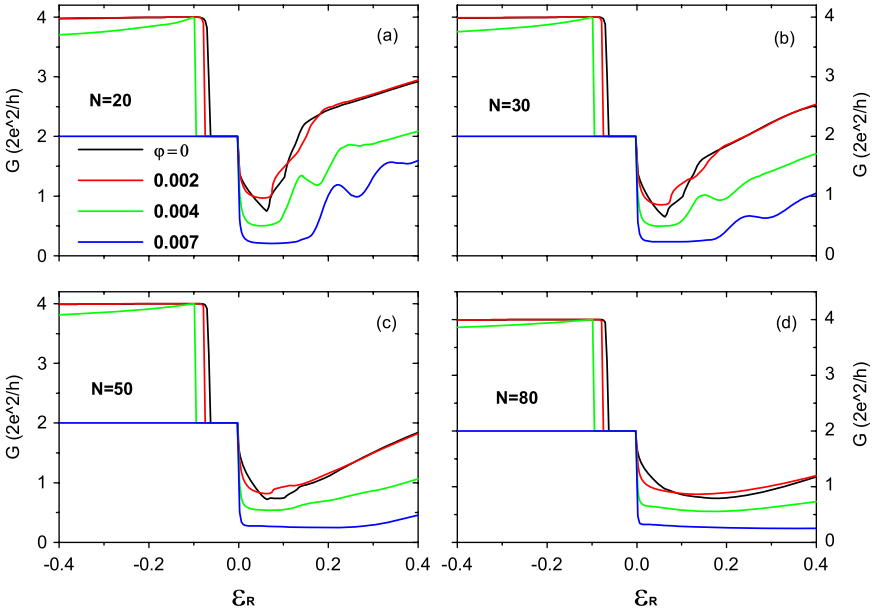

Figure 4. G versus ε_R in a clean BLG p–n junction for different magnetic fields and $M = 30$, $\varepsilon_L = -0.1$.

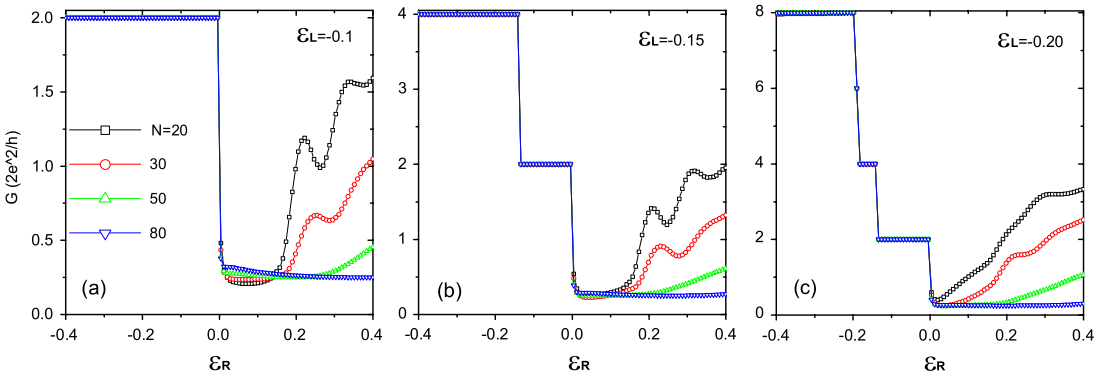

Figure 5. G versus ε_R in a clean BLG p–n junction. The other parameters are $M = 30$ and $\varphi = 0.007$.

e/h). When magnetic field is applied, Landau levels are formed and the Klein tunneling occurs between edge states at the edges of the ribbon instead of along the interfaces between terminals and the central area. The conductance in the n–n region is slightly decreased because the mismatch of discrete Landau levels weakens the Klein tunneling effect (see figure 4(a)). For rather large φ, the number of Landau levels below the Fermi energy is decreased and then the conductance is decreased accordingly. In the p–n regime, the conductance, contributed by edge states, is decreased as a result of Landau level mismatch and decrease of Landau level number below the Fermi energy as well. In figures 4(b)–(d), when the length of the central region becomes large, the Klein tunneling is weakened. The conductance in the n–n regime still maintains its quantized value. Meanwhile in the p–n regime, the conductance is decreased to a small value as a result of the weakened Klein tunneling effect.

To investigate the effect of filling factors in the n- and p-regime on conductance, in figure 5, we show the G versus E for different ε_L values and lengths N. Similarly to an MLG p–n junction, in the n–n region, perfect conductance plateaus in the quantum Hall regime are realized with values $G = \frac{e^2}{h}\min\{|\nu_L|, |\nu_R|\}$. In the p–n region, the conductance is small. For low filling factors (e.g. figure 5(a) $\nu_L = \nu_R = 4$), the longer the central region becomes, the larger the conductance becomes. However, for high filling factors (e.g., $\nu_L\nu_R = 8$ in figures 5(a)–(c)), by contrast, the longer the central region becomes, the smaller the conductance becomes. There is a competition between Klein tunneling and the band selective rule between subbands of two separate BLG terminals [26]. At low filling factors (ν_L, ν_R), the energy discrepancy between two BLG terminals is small and then charges belonging to the first Landau level can tunnel through the junction as a result of the band selection rule. In this situation, Klein tunneling is weak. As the central region becomes longer, charges from the left terminal can transport to the right terminal by way of energy levels in the central region more easily. However, if the energy discrepancy between two BLG terminals is large (Klein tunneling has a remarkable function), according to the band selection rule, charges from the left terminal can hardly

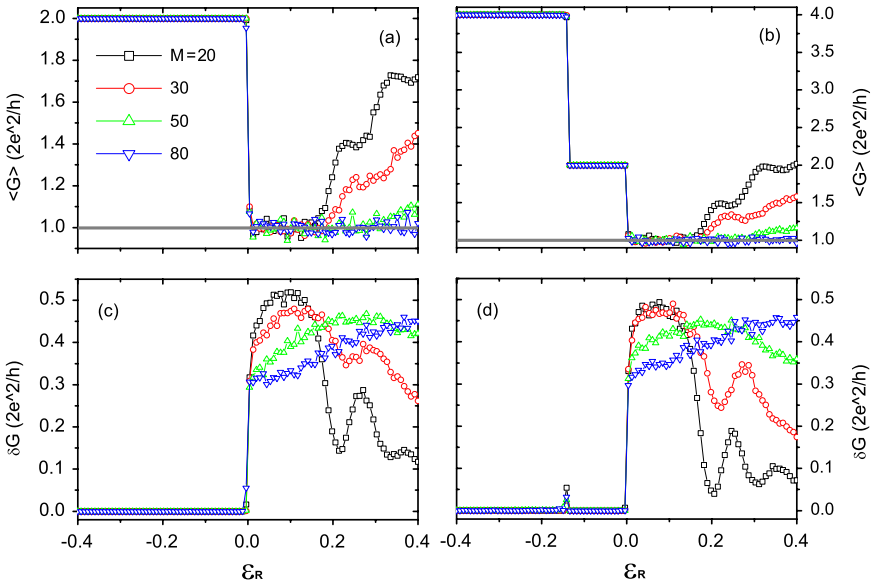

Figure 6. $\langle G\rangle$ versus ε_{R} in a BLG p–n junction with electron–hole inhomogeneity. The other parameters are $M = 30$, $\varphi = 0.007$, $\varepsilon_{\mathrm{L}} = -0.1$ for (a) and (c), $\varepsilon_{\mathrm{L}} = -0.15$ for (b) and (d). The gray straight lines in (a) and (b) are 1.0.

tunnel to the right part. If the central region is longer, Klein tunneling is greatly diminished and hence the conductance becomes smaller.

We now discuss a BLG p–n junction with electron–hole inhomogeneity. In the n–n region, the conductance plateaus are unchanged with values decided by $\langle G\rangle = \frac{e^2}{h}\min\{|\nu_{\mathrm{L}}|, |\nu_{\mathrm{R}}|\}$. However, in the p–n junction, $\langle G\rangle$ is greatly enhanced and a quantized conductance plateau is formed at $2e^2/h$. The plateau can survive for a short junction with low filling factors and for a long junction no matter whether the filling factors are low or not. For a short junction, the conductance is large at high filling factors as a result of Klein tunneling. For longer junctions (e.g. $N = 80$), Klein tunneling is weak and $\langle G\rangle = 2e^2/h$. In figures 6(b) and (d), δG is almost zero in the n–n region which is similar to the MLG situation. In the p–n region, the δG plateau cannot be realized.

3.3. Conductance distribution

From the above discussion, we can notice that the conductance behaviors of MLG and BLG p–n junctions with Anderson disorder and charge puddle disorder are quite different. However, the same plateau $\langle G\rangle = e^2/h$ can be realized in the two disorder models of an MLG p–n junction. Thus we investigate the conductance distribution for both disorder models. In detail, we focus on the conductance distribution in MLG and BLG p–n junctions near the Dirac point. We set a small but positive E and calculate the conductance with 5000 random configurations. First we investigate MLG (figures 7(a) and (b)) and BLG (figures 7(c) and (d)) p–n junctions without magnetic field applied in two cases: Anderson model ((a) and (c)) and charge puddle model ((b) and (d)). It can easily be observed that in both cases, the distribution of G is subject to a Gaussian distribution. The mean value of the conductance is not an integer times e^2/h; it can also be revealed by figure 5 that a conductance plateau cannot be formed if no magnetic field is applied.

Next we investigate the conductance in the quantum Hall regime with $\varphi = 0.007$. First we have to mention that when the conductance is not a quantized one (a plateau or a value given by $\frac{2e^2}{h}\frac{\nu_{\mathrm{L}}\nu_{\mathrm{R}}}{\nu_{\mathrm{L}}+\nu_{\mathrm{R}}}$) and a conductance plateau is not realized, the corresponding conductance distribution has no particular characteristics (not shown here). However, when a quantized conductance plateau is formed, the distributions are subject to a special form (see figure 8). Similar to figure 7, we have studied the MLG (figures 8(a) and (b)) and BLG ((c) and (d)) p–n junctions in two cases: Anderson model ((a) and (c)) and charge puddle model ((b) and (d)). One general characteristic in figure 8 reveals that although the distributions of conductance are different from (a) to (d), they are all symmetric with respect to e^2/h ((a) and (b)) or $2e^2/h$ ((b) and (d)). This characteristic guarantees that the mean values of the conductances are e^2/h or $2e^2/h$, which is also a result obtained from figures 4 and 5. In the case of the Anderson disorder model, the conductance distribution of the MLG p–n junction is uniform (see figure 8(a)) with the probabilities $P(G) = 1$ in the whole interval $[0, e^2/h]$. In the case of the charge puddle model, the conductance distribution function cannot be easily given. They have one similarity that the probability reaches its minimum value at the symmetric center. However, in the case of an MLG p–n junction, $P(G)$ obtained its maximum value at the edges of the interval, and for the BLG p–n junction, $P(G) = 0$ at the edges of the interval.

3.4. $\langle G\rangle$ versus W relation

Finally we discuss how the magnitude of charge puddle disorder strength affects the conductance in an MLG p–n junction. The main results are shown in figure 9. In the n–n region the conductance can survive for disorder strengths over 0.1 (e.g. $\nu_{\mathrm{L}} = \nu_{\mathrm{R}} = -2$ and -6). In the p–n region, the

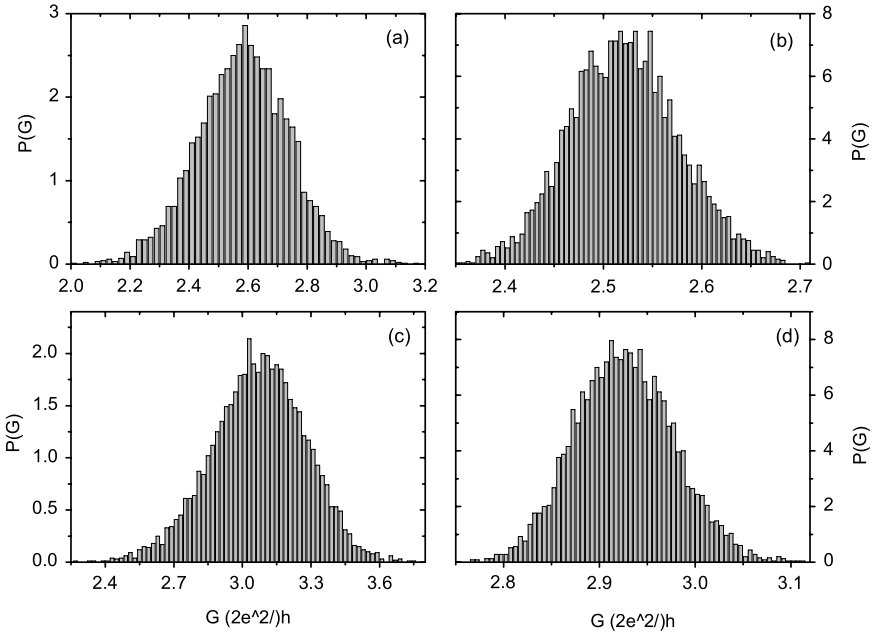

Figure 7. Conductance distribution in an MLG p–n junction ((a) and (b)) and a BLG p–n junction ((c) and (d)) when $\varphi = 0$ with two types of disorder: Anderson disorder ((a) and (c)) and charge puddle ((b) and (d)). The other parameters are $\varepsilon_L = -0.1$, $\varepsilon_R = 0.1$, $M = 50$, $N = 20$, $\varphi = 0$ and $E \approx 0$ but $E > 0$. For the Anderson disorder model, $W = 1$, and for the charge puddle model, $W = 30$ meV.

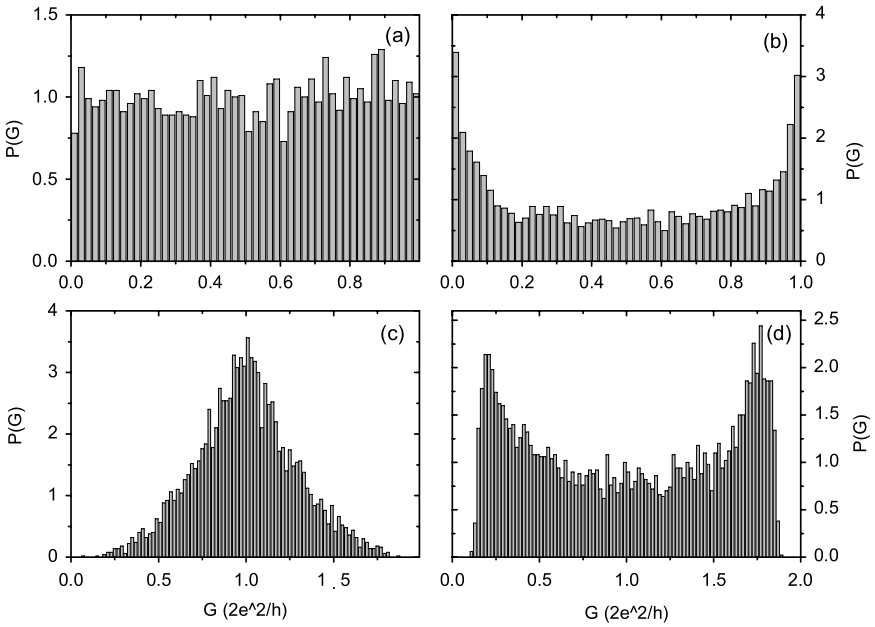

Figure 8. Same as figure 6 with $\varphi = 0.007$.

lowest conductance plateau can be realized in a very small puddle strength ($W = 0.01$ for $\nu_L = -2$ and $\nu_R = 2$). This plateau could survive for over two orders of magnitude of disorder strength $W \in [0.01, 2]$. This interval is much wider than the Anderson disorder model and the lowest magnitude of strength for the realization of the conductance plateau is ten times smaller than that of the Anderson disorder model. For other higher filling factors, corresponding conductance plateaus can be realized for proper disorder strengths. For instance, $\langle G \rangle = 3e^2/2h$ for $\nu_L = -2, \nu_R = 6$ and $\langle G \rangle = 3e^2/h$ for $\nu_L = -6, \nu_R = 6$. However, in experiment, the energy of the puddle is found to be around 30 meV which corresponds to $W \approx 0.01$, thus conductance plateaus at high filling factors are hard to realize.

4. Conclusion

We theoretically study the conductance of an MLG based p–n junction and a BLG p–n junction with electron–hole puddles in the quantum Hall regime. We find that in the presence

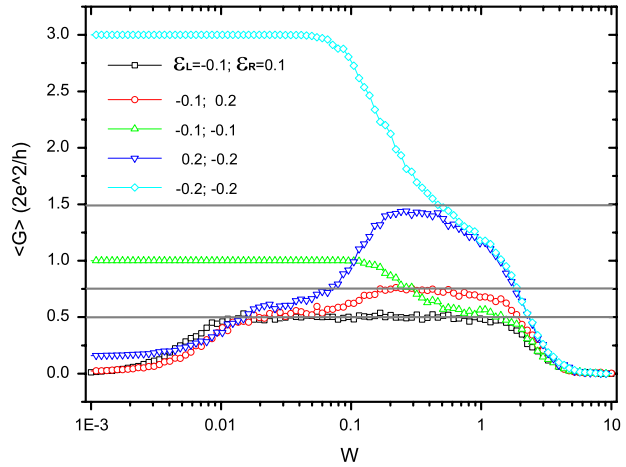

Figure 9. $\langle G \rangle$ in an MLG p–n junction with puddle disorder as a function of disorder strength W (W corresponding to σ in a normal distribution). The gray lines indicate 0.5, 0.75 and 1.5. The other parameters are $M = 30$, $N = 20$ and $\varphi = 0.007$.

of electron–hole inhomogeneity, the quantized conductance plateau of an MLG p–n junction emerges at e^2/h. For a BLG p–n junction, the conductance is enhanced when charge puddles are considered, and the lowest conductance plateau emerges at $2e^2/h$. A universal conductance fluctuation is found to be $2e^2/3h$ in an MLG p–n junction if an ideal conductance plateau is formed. We also investigate the conductance distribution of MLG and BLG p–n junctions where two disorder models are considered in two cases: with and without external magnetic field. We find that if there is no magnetic field, the conductance is subject to a Gaussian distribution. If a large perpendicular magnetic field B is applied, the conductances distributions are different from each other. However, in all cases the distributions of conductances in the quantum Hall regime are symmetric with respect to the mean value which is an integer times e^2/h. Finally we discuss the influence of charge puddle disorder on the conductance of an MLG p–n junction. We find that high conductance plateaus at high filling factors can only be realized under huge disorder strength which is not realistically accessible in experiments.

Acknowledgments

We gratefully acknowledge the financial support from NSF-China under grant No. 11004159 and Natural Science Basic Research Plan in Shaanxi Province of China (No. 2010JQ1007).

References

[1] Novoselov K S, Geim A K, Morozov S V, Jiang D, Zhang Y, Dubonov S V, Grigorieva I V and Firsov A A 2004 *Science* **306** 666
Geim A K and Novoselov K S 2007 *Nat. Mater.* **6** 183
[2] Novoselov K S, Geim A K, Morozov S V, Jiang D, Katsnelson M I, Grigorieva I V, Dubonos S V and Firsov A A 2005 *Nature* **438** 197
[3] Ando T 2005 *J. Phys. Soc. Japan* **74** 777
Castro Neto A H, Guinea F, Peres N M R, Novoselov K S and Geim A K 2009 *Rev. Mod. Phys.* **81** 109
Peres N M R 2009 *J. Phys.: Condens. Matter* **21** 095501
[4] Katsnelson M I, Novoselov K S and Geim A K 2006 *Nat. Phys.* **2** 620
[5] Cheianov V V, Fal'ko V and Altshuler B L 2007 *Science* **315** 1252
[6] Setare M R and Jahani D 2010 *J. Phys.: Condens. Matter* **22** 245503
[7] Zhang Y, Tan Y-W, Stormer H L and Kim P 2005 *Nature* **438** 201
[8] Novoselov K S, Jiang Z, Zhang Y, Morozov S V, Stormer H L, Zeitler U, Maan J C, Boebinger G S, Kim P and Geim A K 2007 *Science* **315** 1379
[9] Harris P J F 2009 *J. Phys.: Condens. Matter* **21** 355009
Castro E V, Novoselov K S, Morozov S V, Peres N M R, Lopes dos Santos J M B, Nilsson J, Guinea F, Geim A K and Castro Neto A H 2010 *J. Phys.: Condens. Matter* **22** 175503
[10] McCann E and Fal'ko V I 2006 *Phys. Rev. Lett.* **96** 086805
Ohta T, Bostwick A, Seyller T, Horn K and Rotenberg E 2006 *Science* **313** 951
[11] Novoselov K S, McCann E, Morozov S V, Fal'ko V I, Katsnelson M I, Zeitler U, Jiang D, Schedin F and Geim A K 2006 *Nat. Phys.* **2** 177
[12] Williams J R, Dicarlo L and Marcus C M 2007 *Science* **317** 638
[13] Li J and Shen S Q 2008 *Phys. Rev.* B **78** 205308
[14] Long W, Sun Q-F and Wang J 2008 *Phys. Rev. Lett.* **101** 166806
[15] Liao Z-M, Han B-H, Zhou Y-B and Yu D-P 2010 *Phys. Lett.* A **374** 3332
[16] Rossi E, Bardarson J H, Brouwer P W and Das Sarma S 2010 *Phys. Rev.* B **81** 121408
[17] Nomura K and MacDonald A H 2007 *Phys. Rev. Lett.* **98** 076602
[18] Hwang E H, Adam S and Das Sarma S 2007 *Phys. Rev. Lett.* **98** 186806
Martin J, Akerman N, Ulbricht G, Lohmann T, Smet J H, von Klitzing K and Yacoby A 2008 *Nat. Phys.* **4** 144
Zhang Y, Brar V W, Girit C, Zettl A and Crommie M F 2009 *Nat. Phys.* **5** 722
[19] Cho S and Fuhrer M S 2008 *Phys. Rev.* B **77** 081402
[20] Deshpande A, Bao W, Zhao Z, Lau C N and LeRoy B J 2009 *Appl. Phys. Lett.* **95** 243502
[21] Meir Y and Wingreen N S 1992 *Phys. Rev. Lett.* **68** 2512
Wingreen N S, Jauho A P and Meir Y 1993 *Phys. Rev.* B **48** 8487
[22] Lee D H and Joannopoulos J D 1981 *Phys. Rev.* B **23** 4997
López-Sancho M P, López-Sancho J M and Rubio J 1984 *J. Phys. F: Met. Phys.* **14** 1205
[23] Ohta T, Bostwick A, McChesney J L, Seyller T, Horn K and Rotenberg E 2007 *Phys. Rev. Lett.* **98** 206802
Malard L M, Nilsson J, Elias D C, Brant J C, Plentz F, Alves E S, Castro Neto A H and Pimenta M A 2007 *Phys. Rev.* B **76** 201401
Yan J, Henriksen E A, Kim P and Pinczuk A 2008 *Phys. Rev. Lett.* **101** 136804
[24] Deshpande A, Bao W, Miao F, Lau C N and LeRoy B J 2009 *Phys. Rev.* B **79** 205411
[25] Koschny Th and Schweitzer L 2003 *Phys. Rev.* B **67** 195307
Kawarabayashi T, Ono Y, Ohtsuki T, Kettemann S, Struck A and Kramer B 2008 *Phys. Rev.* B **78** 205303
Kawarabayashi T, Hatsugai Y and Aoki H 2009 *Phys. Rev. Lett.* **103** 156804
[26] Chen J-C, Cheng S-G, Shen S-Q and Sun Q-F 2008 *J. Phys.: Condens. Matter* **22** 035301